CHAPTER 7

7.1

(a) The in and out movement of the majority carriers about the steady-state depletion width in response to the applied a.c. signal.

(b)

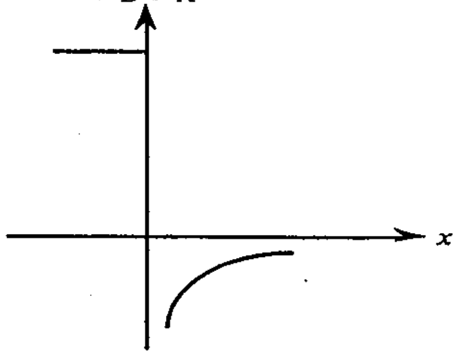

(c) *Quasistatically* is an adverb used to describe a situation where carriers or a device subject to non-steady-state conditions responds as if steady-state conditions applied at each instant of time.

(d) *Varactor*—a contraction of *var*iable re*actor*. A commercial device, such as a reverse-biased *pn* junction diode, where the reactance = $1/j\omega C$ varies as a function of the applied voltage.

(e) *Profiling*—the process of determining the doping concentration inside a device as a function of position.

(f) The low-frequency conductance of an ideal diode was noted to be (Eq. 7.15),

$$G_0 = \frac{q}{kT}(I + I_0)$$

$G_0 \propto I$ when the diode is forward biased and vanishes for reverse biases greater than a few kT/q. Also note that $G_0 = qI_0/kT$ when $V_A = 0$. We conclude

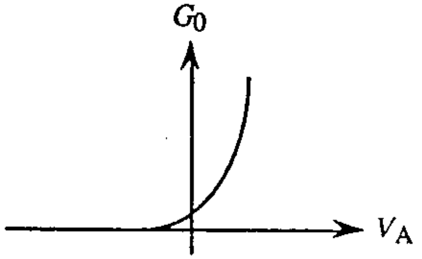

(g) The diffusion admittance arises from fluctuations in the number and position of minority carriers stored in the quasineutral regions adjacent to the depletion region.

(h) At signal frequencies where $\omega\tau_p \gtrsim 1$, the minority carriers have trouble following the a.c. signal and the resulting out-of-phase oscillations enhance the diffusion conductance at the expense of the diffusion capacitance.

7.2

Given

$$N_B(x) = N_D(x) = bx^m \qquad \ldots x > 0$$

the application of the depletion approximation yields

$$\rho \cong qN_D = qbx^m \qquad \ldots 0 \le x \le x_n \cong W$$

Next substituting into Poisson's equation gives

$$\frac{d\mathcal{E}}{dx} = \frac{\rho}{K_S\varepsilon_0} = \frac{qb}{K_S\varepsilon_0}x^m \qquad \ldots 0 \le x \le W$$

Separating variables and solving for the electric field, we find

$$\int_{\mathcal{E}(x)}^{0} d\mathcal{E}' = \int_x^W \frac{qb}{K_S\varepsilon_0}x'^m dx'$$

or

$$-\mathcal{E}(x) = \frac{dV}{dx} = \frac{qb}{K_S\varepsilon_0}\frac{(x')^{m+1}}{m+1}\bigg|_x^W = \frac{qb}{(m+1)K_S\varepsilon_0}(W^{m+1} - x^{m+1})$$

Again separating variables and this time integrating across the entire depletion region, we obtain

$$\int_0^{V_{bi}-V_A} dV = \frac{qb}{(m+1)K_S\varepsilon_0}\int_0^W [W^{m+1} - x^{m+1}]\, dx$$

or

$$V_{bi}-V_A = \frac{qb}{(m+1)K_S\varepsilon_0}\left[W^{m+1}x - \frac{x^{m+2}}{m+2}\right]\bigg|_0^W$$

Note that the second term on the right hand side of the $V_{bi}-V_A$ expression blows up when evaluated at the lower limit if $m < -2$. The solution likewise blows up at the upper limit if $m = -2$. It is for this reason that we must restrict m to values $m > -2$. With $m > -2$, we conclude

$$V_{bi}-V_A = \frac{qb}{(m+1)K_S\varepsilon_0}\left[W^{m+2} - \frac{W^{m+2}}{m+2}\right] = \frac{qb}{(m+2)K_S\varepsilon_0}W^{m+2}$$

or

$$\boxed{W = \left[\frac{(m+2)(K_S\varepsilon_0)}{qb}(V_{bi}-V_A)\right]^{1/(m+2)}}$$

7.3

(a)/(b) Script of a MATLAB program yielding fully-dimensioned reverse-bias C–V curves, and a sample output to be compared with Fig. 7.3, are reproduced below. Using a computed V_{bi} consistent with the specified doping yields capacitance values that are too low. This is especially true at small applied voltages where $|V_A|$ is comparable to V_{bi}. For example, at $V_A = 0$, the computed C_J is 106 pF while the observed value is approximately 123 pF. The noted discrepancy is indeed related to the result in Exercise 7.2 where a lower V_{bi}, a V_{bi} not consistent with the doping concentration, was deduced from the Fig. 7.3 experimental data. Not surprisingly, if one employs the V_{bi} deduced in Exercise 7.2 instead of the computed value (which is possible with the supplied m-file), one obtains excellent agreement with the Fig. 7.3 data. (It should be noted that even better agreement is obtained if 2 pF are added to the computed values to account for stray capacitance.)

(c) Because the depletion width at a given reverse bias shrinks with increased doping, the capacitance, which is proportional to $1/W$, increases with increased doping on the lightly doped side of the junction. This is readily verified by simply running the P_07_03.m program with different N_D inputs.

MATLAB program script...

```
% Fully-dimensioned Reverse-bias C-V curves
% appropriate for p+-n step junction diodes

%Initialization
clear;  close

%Constants and Parameters
q=1.6e-19;  e0=8.85e-14;
EG=1.12;    kT=0.0259;
ni=1.0e10;  KS=11.8;
```

```
s=menu('CHOOSE Vbi APPROACH','Compute','Input');
A=input('Input the diode area in cm^2,  A = ');
ND=input('Input the n-side (of p+-n) doping,  ND = ');
VAmax=input('Input reverse-bias |VA|max,  |VA|max = ');
if s==1,    Vbi=EG/2+kT*log(ND/ni);
else        Vbi=input('Input Vbi,  Vbi = ');
end

%C-V Computation
VA=linspace(0,-VAmax);
CJ0=(KS*e0*A)/sqrt(2*KS*e0*Vbi/(q*ND));
CJ=CJ0./sqrt(1-VA/Vbi);

%Plot result
ymax=1.2*max(CJ);
plot(VA,CJ);
axis([-VAmax,5,0,ymax]);  grid
xlabel('VA (volts)');  ylabel('CJ (pF)')
```

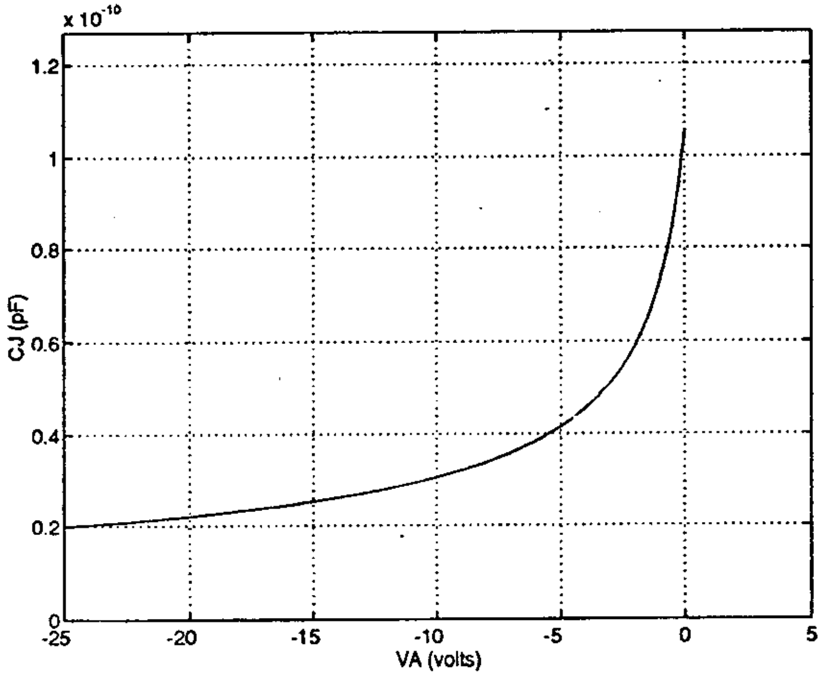

7.4

For an abrupt p^+-n junction, we know in general from Eq. (7.11) that

$$\frac{1}{C_J^2} = \frac{2}{qN_D K_S \varepsilon_0 A^2}(V_{bi} - V_A)$$

After reducing all capacitance values in Table P7.4 by 3pF to account for the stray capacitance shunting the encapsulated diode†, a least squares fit to the corrected data employing the MATLAB polyfit function yields

$$\frac{1}{C_J^2} = (8.254 \times 10^{20}) - (1.123 \times 10^{21})V_A \qquad \text{... } C_J \text{ in Farads}$$

We therefore conclude

$$N_D = \frac{2}{qK_S\varepsilon_0 A^2|\text{slope}|} = \frac{2}{(1.6\times10^{-19})(11.8)(8.85\times10^{-14})(6\times10^{-3})^2(1.123\times10^{21})}$$

$$= \mathbf{2.96 \times 10^{14}/cm^3}$$

and

$$V_{bi} = \frac{8.254\times10^{20}}{1.123\times10^{21}} = \mathbf{0.735\ \ V}$$

Referring to Fig. E5.1, one finds the V_{bi} result here is reasonably close to the theoretically computed $V_{bi} = 0.83$V associated with an $N_D \cong 3 \times 10^{14}/\text{cm}^3$ p^+-n step junction.

† It was incorrectly stated in the first printing of the text that the data listed in Table P7.4 had already been corrected to account for the cited stray capacitance.

A plot of the corrected $1/C_J^2$ versus V_A data, which may be used for obtaining a result by "eyeballing," is displayed below. (Also see m-file P_07_04.m available on the instructor's disk.)

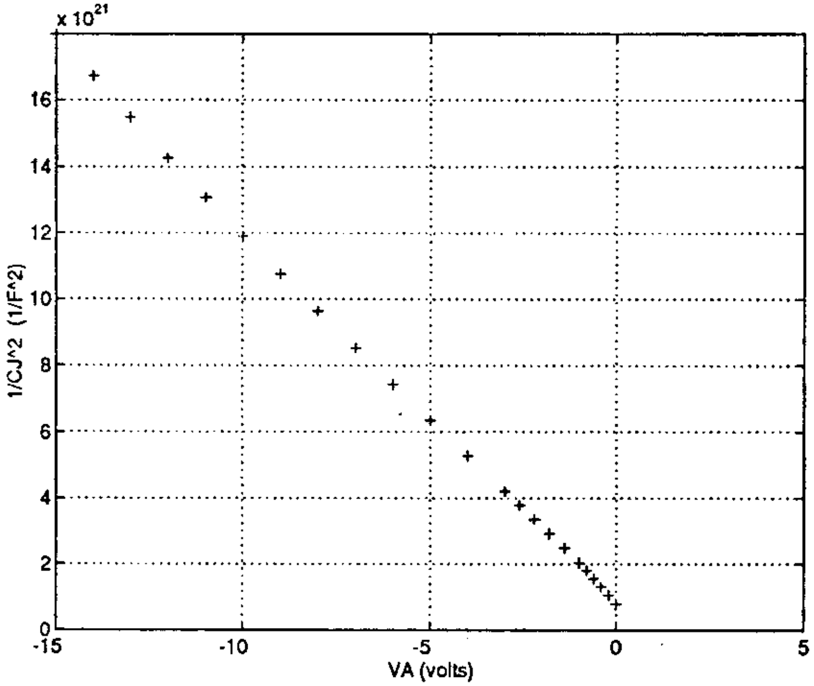

7.5

For concreteness, we take the device under test to be a p^+-n junction diode, with $N_D(x)$ the arbitrary nondegenerate donor doping on the lightly doped side of the junction. Based on the depletion approximation, the total charge in the depletion region on the n-side of the junction will be

$$Q_N = A\int_0^{x_n \cong W} \rho(x)dx = qA\int_0^{W} N_D(x)dx$$

Assuming the diode follows the applied a.c. signal quasistatically,

$$C_J = \frac{dQ_P}{dV_A} = -\frac{dQ_N}{dV_A} = -qA\frac{d}{dV_A}\int_0^{W} N_D(x)dx = -qAN_D(W)\frac{dW}{dV_A}$$

However,

$$C_J = \frac{K_S\varepsilon_0 A}{W}$$

$$\frac{dC_J}{dV_A} = -\frac{K_S\varepsilon_0 A}{W^2}\frac{dW}{dV_A}$$

and therefore

$$\frac{dW}{dV_A} = -\frac{W^2}{K_S\varepsilon_0 A}\frac{dC_J}{dV_A} = -\frac{K_S\varepsilon_0 A}{C_J^2}\frac{dC_J}{dV_A}$$

Substituting back into the generalized capacitance expression then yields

$$C_J = -qAN_D(W)\frac{dW}{dV_A} = \frac{qK_S\varepsilon_0 A^2 N_D(W)}{C_J^2}\frac{dC_J}{dV_A}$$

and solving for $N_D(W)$ gives

$$N_D(W) = \frac{1}{qK_S\varepsilon_0 A^2\left[(dC_J/dV_A)/C_J^3\right]}$$

Finally, noting

$$\frac{d}{dV_A}\left(\frac{1}{C_J^2}\right) = -\frac{2}{C_J^3}\frac{dC_J}{dV_A}$$

and realizing W is synonymous with the distance x from the junction being probed, we obtain

$$N_D(x) = \frac{2}{qK_S\varepsilon_0 A^2\left|d(1/C_J^2)/dV_A\right|}$$

where

$$x = W = \frac{K_S\varepsilon_0 A}{C_J} \qquad \text{... (from } C_J = K_S\varepsilon_0 A/W)$$

7.6 (Solution not supplied.)

7.7

As deduced by combining Eqs. (7.29) and (7.30),

$$G_D/G_0 = \frac{1}{\sqrt{2}}\left(\sqrt{1+\omega^2\tau_p^2}+1\right)^{1/2}$$

$$C_D/C_{D0} = \frac{\sqrt{2}}{\omega\tau_p}\left(\sqrt{1+\omega^2\tau_p^2}-1\right)^{1/2}$$

Computations based on the above relationships and implemented using the program listed below yield an almost perfect reproduction of the text plot.

MATLAB program script...

```
% Frequency variation of the normalized diffusion
% conductance (GD/G0) and capacitance (CD/CD0)
% (reproduction of Fig. 7.10)
%Initialization
clear;  close
%Computation
x=logspace(-2,2);
Gratio=sqrt(sqrt(1+x.^2)+1)./sqrt(2);
Cratio=sqrt(sqrt(1+x.^2)-1).*(sqrt(2)./x);
%Plot
loglog(x,Gratio,x,Cratio);
axis([0.01,200,0.1,20]);  grid
xlabel('angular frequency * lifetime')
text(2.4,2.2,'GD/G0')
text(2.2,0.45,'CD/CD0')
```

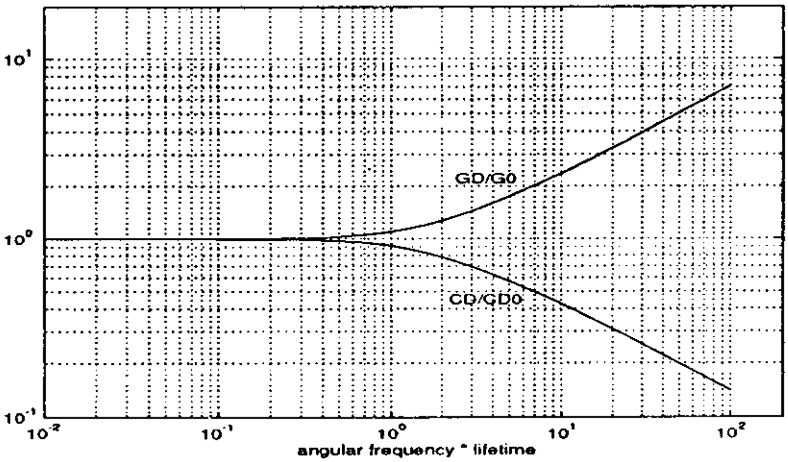

7.8
As deduced by combining Eqs. (7.30a) and (7.30b),

$$\omega C_D/G_D \rightarrow \omega\tau_p/2 \qquad \ldots\ \omega\tau_p << 1$$

As deduced from Eqs. (7.29a) and (7.29b),

$$C_D \rightarrow \frac{G_0}{\omega\sqrt{2}}\sqrt{\omega\tau_p} \qquad \ldots\ \omega\tau_p >> 1$$

$$G_D \rightarrow \frac{G_0}{\sqrt{2}}\sqrt{\omega\tau_p} \qquad \ldots\ \omega\tau_p >> 1$$

and

$$\omega C_D/G_D \rightarrow 1 \qquad \ldots\ \omega\tau_p >> 1$$

In general, again referring to Eqs. (7.29),

$$\frac{\omega C_D}{G_D} = \left(\frac{\sqrt{1+\omega^2\tau_p^2}-1}{\sqrt{1+\omega^2\tau_p^2}+1}\right)^{1/2}$$

A plot of $\omega C_D/G_D$ versus $\omega\tau_p$ that is consistent with the limiting-case solutions and the script of the generating MATLAB program are displayed below. The result here provides some food for thought. Even though G_D increases and C_D decreases with increased frequency above $\omega\tau_p = 1$, the relative size of the real and imaginary components of the diffusion admittance approach the same value and increase at the same rate if $\omega\tau_p >> 1$. Also, the result emphasizes that the diffusion conductance is the larger admittance component at low frequencies.

MATLAB program script...

```
% Relative size of the capacitive and conductive
% components of the diffusion admittance (wCD/GD)

%Initialization
clear; close

%Computation
x=logspace(-2,2);
ratio=sqrt((sqrt(1+x.^2)-1)./(sqrt(1+x.^2)+1));

%Plot
loglog(x,ratio);
axis([0.01,200,0.001,2]); grid
xlabel('angular frequency * lifetime')
ylabel('wCD/GD...w=angular frequency')
```

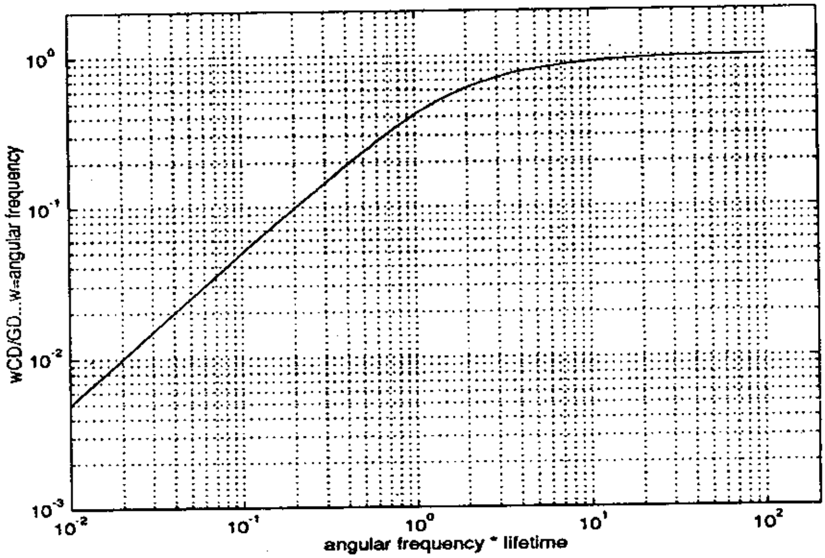

7.9

A table listing the computational variables and the deduced values of τ_n is presented below. Capacitance entries in this table were established as follows:

(1) The $C_{TOTAL} = C_J + C_D$ data spanning the voltage range from 0.5V to 0.58V were extracted from line 20 of the MATLAB program script in Exercise 7.4.

(2) C_J was computed using

$$C_J = C_{J0}/\sqrt{1 - V_A/V_{bi}} = 120/\sqrt{1 - V_A/0.7} \qquad \text{(pF)}$$

The values of C_{J0} and V_{bi} were noted from entries in the Exercise 7.4 program script.

(3) $C_D = C_{TOTAL} - C_J$

V_A (volts)	C_{TOTAL} (pF)	C_J (pF)	C_D (pF)	G_D (S)	$\tau_n = 2C_D/G_D$ (sec)
0.5	276	224	52	2.00×10^{-4}	5.20×10^{-7}
0.52	346	237	109	3.90×10^{-4}	5.59×10^{-7}
0.54	440	251	189	7.15×10^{-4}	5.29×10^{-7}
0.56	654	268	386	1.33×10^{-3}	5.81×10^{-7}
0.58	938	290	648	2.28×10^{-3}	5.68×10^{-7}

$\boxed{\overline{\tau_n} = 5.51 \times 10^{-7} \text{ sec}}$